to be published in *Zeitschrift fuer Anorganische und Allgemeine Chemie.*

(b) Vladimír Balek, "Rare-Gas Diffusion, Reactivity and Electrical Conductivity of Solid ZnO"; to be published in *Physica Status Solidi.*

[12] J. Beretka and M. J. Ridge, "Formation of Zinc Ferrite at Low Temperatures," *Nature (London),* **216** [5114] 473–74 (1967).

[13] Vladimír Balek, "Emanation Method for Estimating Reactivity of Ferric Oxides Prepared from Different Sources," *J. Appl. Chem.,* **20** [3] 73 (1970).

[14] Čestmír Jech and Roger Kelly, "Bombardment-Induced Disorder: I," *J. Phys. Chem. Solids,* **30** [3] 465–74 (1969).

[15] (a) S. Malčić, Lj. Petrović, and S. J. Kiss, "X-Ray Investigation of Nickel-Zinc Ferrite Formation," *Bull. Boris Kidric Inst. Nucl. Sci., Ceram. Met.,* **20** [1] (1969).

(b) D. Cerović, I. Momčilović, and S. J. Kiss; pp. 443–46 in Proceedings of the Vth International Congress on X-Ray Optics and Microanalysis, Tubingen 1968. Edited by G. Möllenstedt and K. H. Gaukler. Springer-Verlag, Berlin, 1969.

[16] P. Reijnen; pp. 562–71 in Reactivity of Solids. Edited by G. M. Schwarb. American Elsevier Publishing Co., Inc., New York, 1965.

[17] Vladimír Balek; Ph.D. Thesis, Moscow State University, 1967.

[18] Vladimír Balek, "Temperature Dependence of Characteristic Properties of α-Fe_2O_3 Powders"; to be published in *Journal of Materials Science.*

[19] (a) Roland Lindner, "Diffusion of Radioactive Zinc in Zinc-Iron Spinel and Zinc Oxide," *Acta Chem. Scand.,* **6** [4] 457–67 (1952).

(b) Roland Lindner, "Formation of Spinels and Silicates by Reactions in the Solid State, Investigated by Method of Radioactive Tracers," *Z. Elektrochem.,* **59** [10] 967–70 (1955).

Stress Corrosion and Static Fatigue of Glass

S. M. WIEDERHORN and L. H. BOLZ

Institute for Materials Research, National Bureau of Standards, Washington, D. C. 20234

Stress corrosion cracking of six glasses was studied using fracture mechanics techniques. Crack velocities in water were measured as a function of applied stress intensity factor and temperature, and apparent activation energies for crack motion were obtained. Data were consistent with the universal fatigue curve for static fatigue of glass, which depended on glass composition. Of the glasses tested, silica glass was most resistant to static fatigue, followed by the low-alkali aluminosilicate and borosilicate glasses. Sodium was detrimental to stress corrosion resistance. The crack velocity data could be explained by the Charles and Hillig theory of stress corrosion. It is probable that stress corrosion of glass is normally caused and controlled by a chemical reaction between the glass and water.
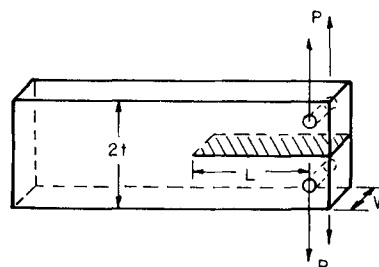
Fig. 1. Specimen configuration. Cross-hatched area designates fracture surface; direction of propagation is from right to left. Web is not shown.

I. Introduction

GLASS is noted for its chemical inertness and general resistance to corrosion; therefore, it is used in the chemical industry and in the laboratory when chemical inertness is required. Despite this well-known property, glass is extremely susceptible to stress corrosion cracking caused by water in the environment.[1-3] This phenomenon is known in the glass literature as static fatigue or delayed failure.

The susceptibility of glass to stress corrosion cracking was observed first by Grenet,[4] who noted a time delay to failure and a loading rate dependence of strength. Although he was unable to explain his observations, subsequent studies have demonstrated that the effect is an activated process caused by water in the environment.[5-9] It is currently believed that static fatigue of glass results from the growth of small cracks in the surface of glass under the combined influence of water vapor and applied load.[1,5,6]

A new method[10-16] for studying the stress corrosion of glass involves measuring the velocity of macroscopic cracks as a

function of external and internal variables such as temperature, applied load, and composition. Basic parameters such as activation energies and volumes may be obtained by this technique. These parameters in turn can be related to other rate processes that may occur at the crack tip during growth and may in fact control the rate of stress corrosion. Thus, information obtained from crack growth studies may be used to describe stress corrosion in terms of fundamental processes such as diffusion and chemical reactions.

The present work is a study of crack growth rates in six glasses tested in water with temperature and applied load as external variables. The data are consistent with the stress corrosion theory of Charles and Hillig[17,18] and with static fatigue data in the form of the universal fatigue curve obtained by Mould and Southwick.[19]

II. Experimental Procedure

The experimental geometry is shown in Fig. 1. The essential experimental parameters are crack length, L; thickness, w; height, $2t$; and applied load, P. Crack propagation was restrained to the midplane by using slotted cantilever specimens 75 by 25 by 1.5 mm in which two slots 0.3 mm deep and 0.1 mm wide were cut along the midplane of the specimen, leaving

Table I.   Glass Composition

Glass	Component (wt fraction)										Annealing temp. (°C)
	SiO₂	B₂O₃	Al₂O₃	Na₂O	K₂O	MgO	CaO	PbO	TiO₂	As₂O₃	
Silica	0.998										
Aluminosilicate I	.57	0.04	0.20	0.01		0.12	0.06				715
Aluminosilicate II	.618		.17	.125	0.034	.036	.004		0.008	0.005	580
Borosilicate	.80	.14	.02	.04							565
Lead-alkali	.60		.04	.10	.02			0.24			470
Soda-lime silicate	.72		.02	.14	.01	.04	.07				528

the halves of the specimen attached by a web 0.9 mm thick. A point of easy crack initiation was provided by cutting away ≈ 1 cm of the web and leaving the end of the web wedge-shaped. A similar geometry was used by Linger and Hollo-way[20] in studying fracture surface energies of glass.

Specimens were glass microscope slides of known composition (Table I). With the exception of the fused silica, specimens were annealed after the slots were cut and cooled 2°C/h until they were 200°C below the annealing point (Table I). It is presumed that the annealing produced identical structures in all specimens of a given composition.

Specimens were mounted in a universal testing machine using two hooks which passed through holes $^1/_{16}$ in. in diameter. Crack motion was observed through a ×20 microscope attached to a cathetometer, allowing the crack length to be measured to ±0.01 cm. The crack surface was illuminated by reflected light. To measure the crack velocity, a filar eyepiece was attached to the microscope and a potentiometer to the eyepiece. By matching the position of the cross hair of the eyepiece to the position of the crack, the motion of the crack could be registered directly on a strip chart recorder. Relative crack length changes measured with the filar eyepiece were accurate to ±0.001 cm; velocities as high as 10^{-4} m/s could be measured. A constant applied load was maintained during each measurement by a spring between the load cell and the specimen. A crack was generated in the web by gradually increasing the applied load. The crack was then forced to grow until L/t was greater than 1.5, at which point experimental measurements of crack velocity were made. Changes in crack length during each velocity measurement ranged from 0.1 to 1% of the original length.

Measurements were conducted in distilled water maintained at 2°, 25°, 40°, 60°, and 90°C. The test container was a 2000 ml beaker. A temperature of 2°C was maintained by floating ice in the water, and the 40°, 60°, and 90°C temperatures were regulated by a heating mantle that completely enclosed the beaker. Temperatures were controlled to ±1°C.

Data are presented as log crack velocity vs the stress intensity factor, K_I. Stress intensity factors were used as variables because they are proportional to the stresses near the crack tip. By using stress intensity factors, crack length and specimen geometry are eliminated as experimental variables; the results obtained using different experimental configurations can then be compared. The stress intensity factor for the notched double cantilever configuration can be calculated from the formula

$$K_I = [PL/(wa)^{0.5}\ t^{1.5}][3.47 + 2.32t/L] \qquad (1)$$

where a is the web thickness and P, L, w, and t are defined in Fig. 1. Equation (1) was obtained by modifying the equations given in Refs. 21 and 22. The meaning and use of stress intensity factors are discussed in Refs. 23–25.

III.   Results

The fracture behavior of four glasses in water at 25°C is shown in Fig. 2; composition has a marked effect on the rate
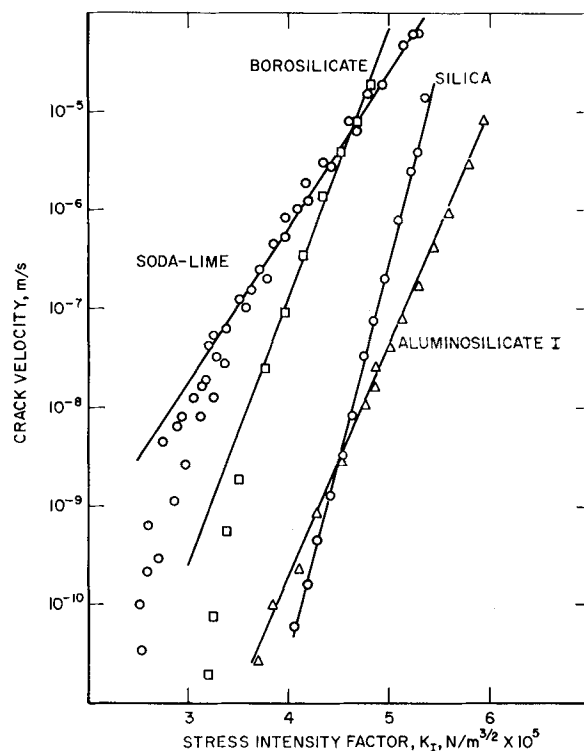

Fig. 2.   Fracture behavior of glass in water at 25°C.

of crack growth. For soda-lime silicate and borosilicate glasses, the crack velocity depends exponentially on the stress intensity factor for velocities greater than 10^{-7} and 10^{-8} m/s, respectively. At slower velocities, the crack velocity decreases at greater than an exponential rate, suggesting a threshold stress intensity below which crack motion does not occur. This threshold is known as the static fatigue limit.[26,27] The aluminosilicate and silica glasses differ from the others in that the behavior is exponential over the entire range of experimental variables; there is no indication in Fig. 2 of a static fatigue limit, although one presumably exists for aluminosilicate and silica glasses at lower stress intensity values.

The influence of temperature on stress corrosion is shown in Fig. 3 for soda-lime silicate glass. The shape of the curve remains the same with changing temperature, but a temperature shift occurs. Also, exponential dependence is obtained over a more limited velocity range as the temperature increases. Thus, the 90°C curve exhibits exponential behavior only to 10^{-6} m/s.

The temperature behavior of all the glass compositions was determined in the exponential range. The data were similar to those for soda-lime silicate glass; however, the slopes and the positions of the curves depended on glass composition. Figure 4 shows the temperature behavior of soda-lime silicate
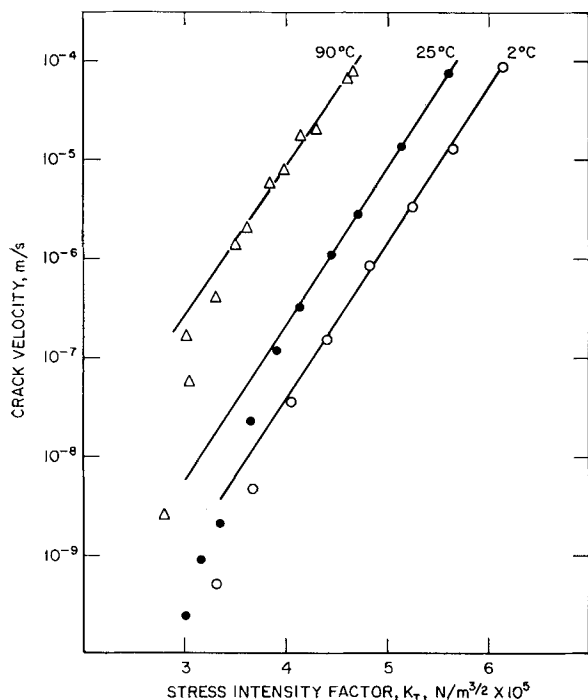
Fig. 3. Influence of temperature on fracture behavior of soda-lime silicate glass in water.

Table II. Summary of Stress Corrosion Data

Glass	E^* (kcal/mol) [*] (J/mol)	b (mks units)	ln v_0
Silica	33.1±1.0 (1.391 E5)	0.216±0.006	−1.32±0.6
Aluminosilicate I	29.0±0.7 (1.212 E5)	.138±0.003	5.5±0.4
Aluminosilicate II	30.1±0.6 (1.262 E5)	.164±0.003	7.9±0.3
Borosilicate	30.8±0.8 (1.288 E5)	.200±0.005	3.5±0.5
Lead-alkali	25.2±1.2 (1.056 E5)	.144±0.006	6.7±0.6
Soda-lime silicate	26.0±1.1 (1.088 E5)	.110±0.004	10.3±0.5

[*] Values given in J/mol in parentheses.

and silica glasses; the curves for other compositions lay between these extremes. Curves were approximately parallel but shifted to higher velocities with increasing temperature. The silica curves are more closely spaced, have greater slopes, and, as a group, are located at higher stress intensity factors than the soda-lime silicate curves.

Data such as those in Fig. 4 can be used to obtain information on the activated processes occurring during stress corrosion cracking. The data were found to fit the equation

$$v = v_0 \exp \left(-E^* + bK_I \right) / RT \qquad (2)$$

where v is the crack velocity and v_0, E^*, and b are experimental constants determined by fitting the data to Eq. (2) by the method of least squares. Since the relative precision of K_I was less than that of log v, the error was minimized in K_I, as discussed in Ref. 28. The experimental constants and their standard deviations are presented in Table II. The apparent activation energy at zero load, E^*, ranged from 25.2 for lead-alkali glass to 33.1 kcal/mol for silica glass with a standard deviation of from 2 to 5% E^*. The stress intensity factor coefficient, b, changed by a factor of nearly 2, ranging from 0.11 for soda-lime silicate glass to 0.216 for silica glass, with the standard deviation varying from approximately 3 to 4% of b. The natural logarithm of the preexponential factor varied from −1.32 for silica glass to 10.2 for soda-lime silicate glass with standard deviations of approximately 0.5.
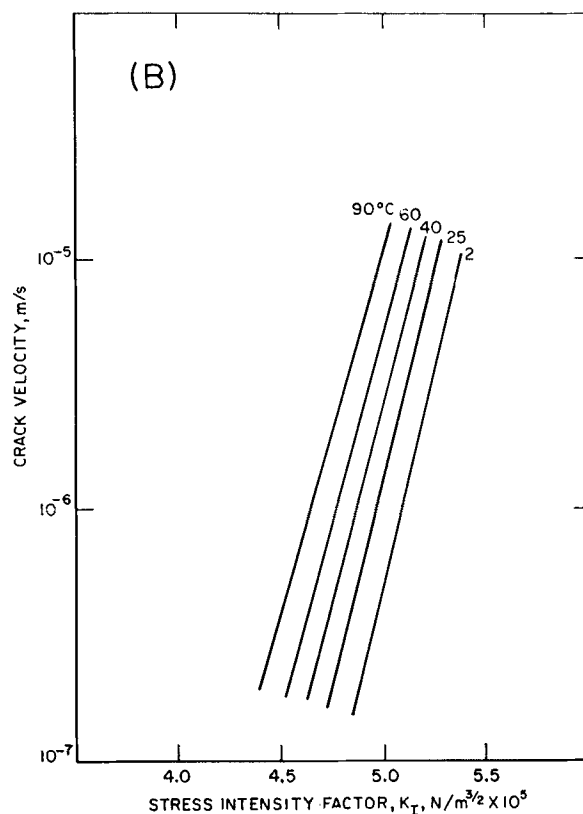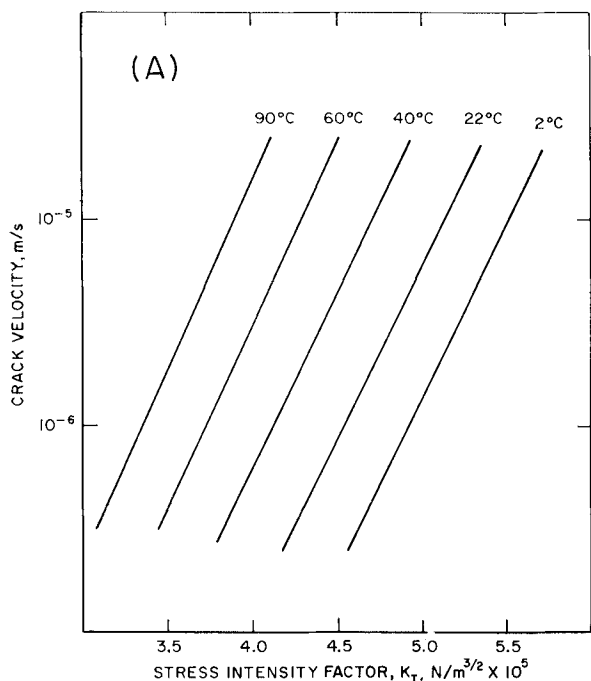

Fig. 4. Exponential stress corrosion behavior of (*A*) soda-lime silicate and (*B*) silica glass in water as a function of temperature.
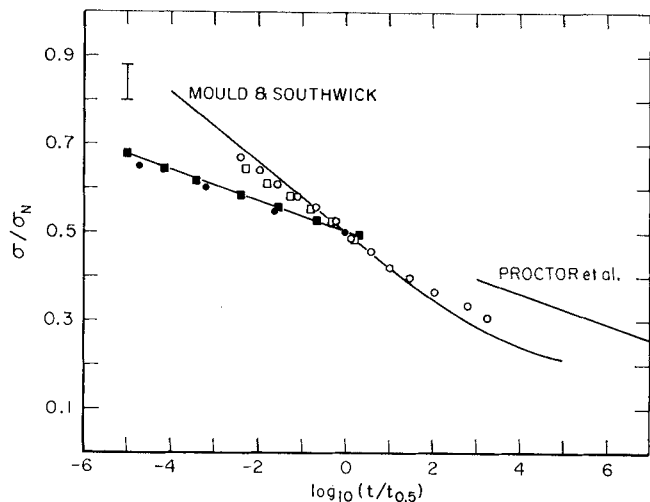
Fig. 5. Crack velocity data compared with universal fatigue curve. Open and closed circles were obtained from Fig. 2 for soda-lime silicate and fused silica glasses, respectively. Open and closed squares were obtained from Table II and Eq. (5) for soda-lime silicate and fused silica glasses, respectively. Curve labeled Mould and Southwick was taken from Ref. 19; error bar gives standard deviation of data associated with this curve. Curve labeled Proctor *et al.* was determined from data in Ref. 29.

IV. Discussion of Results

(1) Comparison of Crack Velocity Data with Universal Fatigue Curve

The strength of glass depends on the presence and growth of small surface cracks, normally less than 10 μm in size. In contrast, the present study gives results for the growth of macroscopic cracks. It is of interest to determine if these results relate to those obtained by the bending and tensile testing techniques. Crack velocity studies and strength studies will now be compared.

One of the most definitive studies of static fatigue of glass was performed by Mould and Southwick.[19] Four-point bend tests in water were conducted on soda-lime silicate glass microscope slides that had received a variety of surface abrasion treatments. Strength vs time-to-failure curves were obtained, each abrasive treatment giving a distinct curve. A single curve fitting all the data could be obtained if the ratio of the strength in air to that in liquid nitrogen, σ/σ_N, were plotted against the logarithm of the reduced time to failure, $\log(t/t_{0.5})$, where $t_{0.5}$, the characteristic duration, is the time to failure of a specimen loaded at half its liquid nitrogen strength. This type of curve, termed the universal fatigue curve, is valuable for theoretical and engineering reasons.

Universal fatigue curves can be calculated from the data presented in Fig. 2 and Table II. Since the stress intensity factor, K, is directly proportional to the applied load, σ, $K/K_{IC} = \sigma/\sigma_N$, where K_{IC} is the critical stress intensity factor for failure in liquid nitrogen. The logarithm of the reduced time to failure, $\log(t/t_{0.5})$, is obtained either by numerical integration of the data in Fig. 2 or by analytical integration of Eq. (2). In either case, a crack geometry must be assumed to provide a relation between applied load, crack size, and stress intensity factor.[23]

To perform the numerical integration, the stress intensity factor is calculated for a crack of initial length, L, and a fixed load condition, and the crack velocity, v, is determined from Fig. 2. The time, Δt, for an incremental increase in length, ΔL, is then determined from $\Delta t = \Delta L/v$, and a new stress intensity factor is calculated from the new crack length, $L + \Delta L$. The process is repeated until $K = K_{IC}$, and the time to failure is equal to the sum of the time increments, $\Sigma \Delta t$.

Analytical integration of Eq. (2) also gives universal fatigue curves. The integration is demonstrated here for a two-dimensional Griffith crack for which $K_I = S\sqrt{\pi L}$, where S is the applied stress and L the half-length of the crack. From Eq. (2), $dt = dL/[v_0 \exp(-E^* + bK_I)/RT]$. Using the relation between stress intensity factor, applied stress, and crack length, the following integrable equation is obtained for the total time to failure:

$$t = [2L/K_I^2 v_0 \exp(-E^*/RT)] \int_{K_I}^{K_{IC}} K \exp(-bK/RT)dK \qquad (3)$$

where K_I is the stress intensity factor calculated from the initial crack length and the applied load. The following equation for the total time to failure is obtained by integrating and neglecting relatively small terms:

$$t = 2RTL/K_I b v_I \qquad (4)$$

where v_I is the initial crack velocity. To the same approximation it can be shown that

$$K_I/K_{IC} = \sigma/\sigma_N = 0.5 - (2.3RT/bK_{IC})\log(t/t_{0.5}) \qquad (5)$$

This is the form of the universal fatigue curve. For a penny-shaped crack, equations identical to Eqs. (3), (4), and (5) are obtained. For the double cantilever configuration, assuming long cracks for which $K_I = 3.47PL/wt^{1.5}$, Eq. (4) is multiplied by 0.5 and Eq. (5) is unchanged. Equation (5) does not describe stress corrosion phenomena for very short failure times or for failure times approaching the fatigue limit. A more complete expression is given by Charles and Hillig.[17,18]

Universal fatigue curves were calculated from Table II and Eq. (5) and by numerical integration of Fig. 2. Results are presented in Fig. 5 for soda-lime silicate and silica glasses. The calculated curves were insensitive to crack geometry and were indistinguishable on the scale of Fig. 5. Slight differences in the curves obtained by the numerical and analytic methods can be attributed to differences in the original crack velocity data. Each of the glasses could be represented by a distinct curve, indicating a sensitivity to composition. The dependence of the universal fatigue curve on composition, noted by Ritter[30] and by Proctor *et al.*[29] from experimental data, is predicted by the theory of Charles and Hillig.[17,18] For soda-lime silicate glass, crack velocity and strength data agree very well, since the calculated data points fall within the scatter band of data obtained by Mould and Southwick.[19] It is also satisfying that the silica glass curve lies in a direct line with data obtained by Proctor *et al.*[29] with silica glass fibers. Thus, the conclusion that crack velocity data are consistent with data obtained from strength studies appears to be justified by the agreement shown in Fig. 5.

(2) Calculation of Static Fatigue Curves from Crack Velocity Data

For engineering purposes, it is useful to have static fatigue curves that are not expressed in terms of reduced variables, since such curves give the actual time to failure at a given load and can be used to judge glass compositions for design purposes. Once the universal fatigue curve for a glass is known, static fatigue curves can be calculated by measuring the liquid nitrogen strength of the glass and the time to failure at half the liquid nitrogen strength. Static fatigue curves can also be calculated from Eq. (4) if b, v_0, and E^* are known. Figure 6 was produced by the latter procedure, assuming that the glasses contained Griffith cracks 10^{-6} m in size. Thus, all the glasses were assumed to contain flaws of equal size. The curves are valid to log $t \approx 3.5$ since this was the range of crack velocity data. The curvature in Fig. 2 was ignored since it was small over the range of times studied. For longer durations, the curvature would be important.
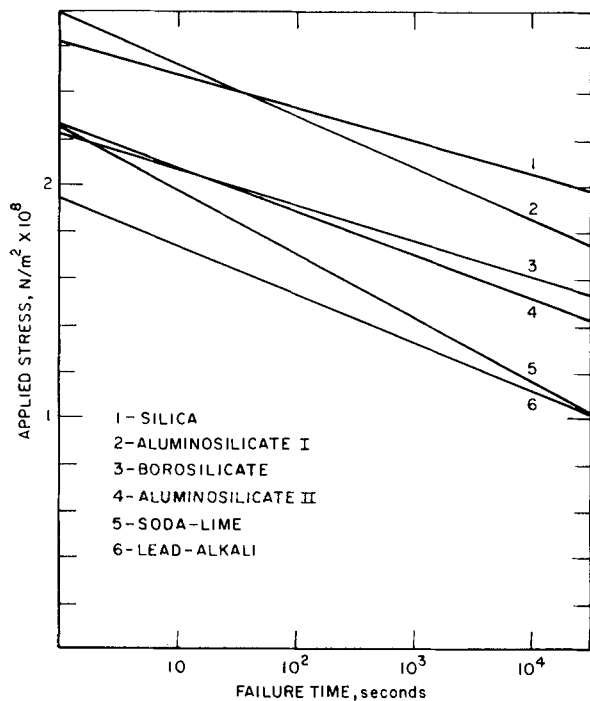
Fig. 6. Static fatigue curves for glass compositions studied. Curves calculated from Eq. (4) using data in Table II.

Fig. 7. Characteristic duration of soda-lime silicate glass subjected to mechanical damage treatments. Data taken from Ref. 19.

Figure 6 shows that fused silica has the greatest stress corrosion resistance for long time loads, whereas the soda-lime silicate and lead-alkali glasses have the poorest resistance. The aluminosilicate I and borosilicate glasses occupy intermediate positions, with aluminosilicate I appearing superior. The behavior seems to be related to the sodium content of the glasses; those which contain large amounts of sodium behave poorly under stress corrosion conditions. As the temperature is increased, the resistance of all the glasses to stress corrosion decreases. The relative positions of the curves of Fig. 6 remain approximately the same, and conclusions concerning the relative merits of the glasses for stress corrosion resistance are unchanged.

(3) Characteristic Durations

The characteristic durations, $t_{0.5}$, calculated from Eq. (4) and those obtained experimentally by Mould and Southwick[19] will now be compared. The characteristic duration is given by Eq. (4) when $K_i = K_{IC}/2$ and $v_i = v_{0.5} = v_0 \exp (-E^* + bK_{IC}/2)/RT$. Except for L, all terms on the right side of Eq. (4) are constants at a given temperature. For a Griffith crack, $K_{IC} = \sigma_N \sqrt{\pi L}$, and for a penny-shaped crack, $K_{IC} = 2\sigma_N \sqrt{L/\pi}$. Substituting these equations into Eq. (4) gives

$$t_{0.5} = (4/\pi) (RTK_{IC}/bv_{0.5}) \sigma_N^{-2} \qquad (6)$$

for the Griffith-type crack and

$$t_{0.5} = \pi (RTK_{IC}/bv_{0.5}) \sigma_N^{-2} \qquad (7)$$

for the penny-shaped crack. The characteristic duration is proportional to the inverse square of the strength in liquid nitrogen, and, for a given strength, the duration of the penny-shaped cracks is greater than that of the Griffith cracks.

The characteristic duration data of Mould and Southwick are presented in Fig. 7. The data are plotted as log $t_{0.5}$ vs log σ_N

---

*Originally, Mould and Southwick plotted their data as log $t_{0.5}$ vs $(1/\sigma_N)^2$.
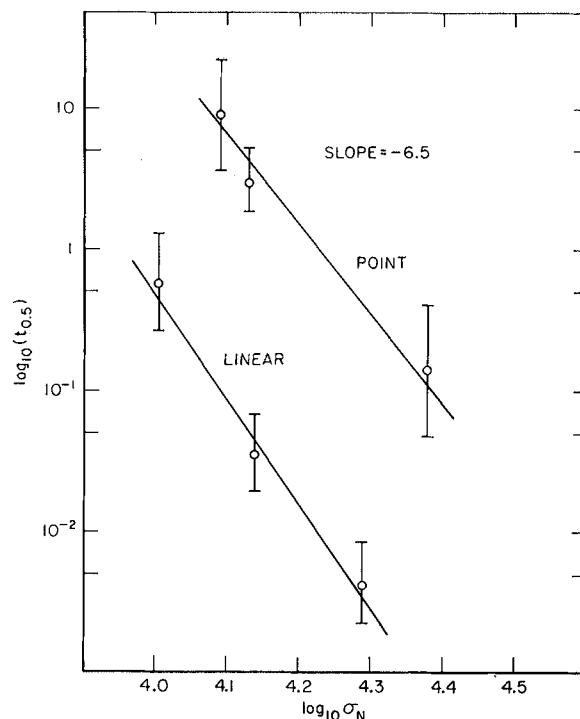
for easy comparison with Eqs. (6) and (7).* As was discussed by Mould and Southwick, different curves are obtained for slides containing point flaws and linear flaws. The slopes of both curves are approximately −6.5; the curve for point flaws lies at longer characteristic durations than the other. If the penny- and Griffith-shaped cracks are assumed to be representative of point and linear flaws, respectively, the displacement of the calculated curves agrees with that found by Mould and Southwick. The slopes of the two sets of data, however, do not agree, since the slope of the experimental data (Fig. 7) is about 3 times that determined from Eqs. (6) and (7). Thus, the measured and calculated durations do not agree quantitatively. Although Eq. (4) may be used to judge the relative resistance of glass to static fatigue qualitatively, it does not predict the failure times quantitatively.

The difference between the calculated and measured characteristic durations may result from differences in the type of cracks studied. Cracks introduced by the techniques used by Mould and Southwick were probably representative of flaws found in real materials and consequently were much more irregular than those studied in the present investigation. It is doubtful that cracks introduced by abrasion or impact are flat or lie perpendicular to the tensile axis. Therefore, the dependence of stress intensity factor on flaw size may differ from those used in the present study. Considering these factors, the measured and calculated characteristic durations might be expected to disagree. The universal fatigue curves seem much less sensitive to these effects, as evidenced by the good agreement obtained in Fig. 5.

(4) Static Fatigue as a Chemical Process

The crack velocity data presented in the present paper agree very well with the stress corrosion theory developed by Charles and Hillig,[17,18] who assumed that static fatigue in glass is controlled by a chemical reaction between the glass and water in the environment. Since chemical reactions are activated processes, static fatigue should also be an activated process. Also,

the activation energy for the process will be stress-sensitive, and the reaction would be expected to occur most rapidly where the stress fields were the greatest. Thus, the water is expected to react most rapidly at the crack tip, extending the crack length until the Griffith conditions for spontaneous failure are satisfied.

Charles and Hillig developed these ideas into a quantitative theory for static fatigue, in which the crack velocity is given by

$$v = v_0 \exp(-E^{\ddagger} + V^{\ddagger}\sigma - V_M\gamma/\rho)/RT \qquad (8)$$

where $E^{\ddagger}$ is the stress free activation energy, $V^{\ddagger}$ the activation volume, σ the stress at the crack tip, V_M the molar volume of the glass, γ the interfacial surface energy between the glass and the reaction products, and ρ the radius of curvature of the crack tip.

Equation (8) was derived for a two-dimensional Griffith crack for which $\sigma = 2K_I/\sqrt{\pi\rho}$. At stresses greater than the fatigue limit, crack sharpening occurs, and ρ decreases to a small value limited by the structure of the glass. Thus, above the static fatigue limit, the third term is a constant independent of applied load, and Eq. (8) takes the form

$$v = v_0 \exp(-E^* + 2V^{\ddagger}K_I/\sqrt{\pi\rho})/RT \qquad (9)$$

where $E^* = E^{\ddagger} + V_M\gamma/\rho$. Depending on the values assumed for γ and ρ, $V_M\gamma/\rho$ ranges from 10 to 20% E^*. Equation (7) is identical to Eq. (2) if $V^{\ddagger} = (b/2)\sqrt{\pi\rho}$. Thus, the observed form of the experimental data for large loads is identical to that predicted from the theory of Charles and Hillig. The bending of the curves for soda-lime silicate and borosilicate glasses at low loads may indicate a change in crack tip radius, a change in rate-limiting mechanism, or an approach to the fatigue limit.

V. Summary

The stress corrosion of glass was studied using fracture mechanics techniques. Crack velocity data were obtained as a function of glass composition, applied stress intensity factor, and temperature. The observed crack velocity data depended strongly on glass composition. The stress corrosion behavior was consistent with static fatigue studies of glass since universal fatigue curves determined from the crack velocity data agreed with those obtained from strength data. Universal fatigue curves depended on glass composition, confirming the observations of other workers. Calculated static fatigue curves could be used to judge which glasses would exhibit good stress corrosion resistance and which would not. Of the glasses studied, silica glass had the greatest stress corrosion resistance, followed by the low-alkali aluminosilicate and borosilicate glasses. Sodium seemed to be detrimental to the stress corrosion resistance of glass. Calculated characteristic durations agreed only qualitatively with those measured by Mould and Southwick for soda-lime silicate glass. The difference in behavior was attributed to differences in crack shape in the experiments. The crack velocity data presented in the present paper agreed with the stress corrosion theory of Charles and Hillig; it is probable that the stress corrosion of glass is caused and controlled by a chemical reaction between water in the environment and the glass.

References

[1] R. J. Charles; pp. 1–38 in Progress in Ceramic Science, Vol. 1. Edited by J. E. Burke. Pergamon Press, New York, 1961.

[2] W. B. Hillig; pp. 152–94 in Modern Aspects of the Vitreous State, Vol. 2. Edited by J. D. Mackenzie. Butterworth Inc., Washington, D. C., 1962.

[3] C. J. Phillips, "Strength and Weakness of Brittle Materials," *Amer. Sci.*, **53** [1] 20–51 (1965).

[4] Louis Grenet, "Mechanical Strength of Glass," *Bull. Soc. Enc. Industr. Nat. Paris* (Ser. 5), **4**, 838–48 (1899).

[5] L. H. Milligan, "Strength of Glass Containing Cracks," *J. Soc. Glass Technol.*, **13** [52] 351–60T (1929).

[6] C. Gurney and S. Pearson, "Effect of Surrounding Atmosphere on Delayed Fracture of Glass," *Proc. Phys. Soc., London, Sect. B*, **62** [356] 469–76 (1949).

[7] T. C. Baker and F. W. Preston, "Fatigue of Glass Under Static Loads," *J. Appl. Phys.*, **17** [3] 170–78 (1946).

[8] T. C. Baker and F. W. Preston, "Effect of Water on Strength of Glass," *ibid.*, pp. 179–88.

[9] R. J. Charles, "Static Fatigue of Glass: I, II," *ibid.*, **29** [11] 1549–60 (1958).

[10] G. R. Irwin, "Moisture Assisted Slow Crack Extension in Glass Plates," NRL Memorandum Report 1678, January 28, 1966.

[11] S. M. Wiederhorn; pp. 503–28 in Materials Science Research, Vol. 3. Edited by W. W. Kriegel and Hayne Palmour III. Plenum Press, New York, 1966.

[12] S. M. Wiederhorn; pp. 293–317 in Environment-Sensitive Mechanical Behavior of Materials. Edited by A. R. C. Westwood and N. S. Stoloff. Gordon and Breach, Science Publishers, Inc., New York, 1966.

[13] S. M. Wiederhorn, "Influence of Water Vapor on Crack Propagation in Soda-Lime Glass," *J. Amer. Ceram. Soc.*, **50** [8] 407–14 (1967).

[14] S. M. Wiederhorn, "Moisture Assisted Crack Growth in Ceramics," *Int. J. Fract. Mech.*, **4** [2] 171–77 (1968).

[15] K. Schonert, H. Umhauer, and W. Klemm, "Influence of Temperature and Environment on Slow Crack Propagation in Glass"; Paper 41, Preprint of Second International Conference on Fracture, Brighton, April 13–18, 1969.

[16] J. A. Kies and A. B. J. Clark, "Fracture Propagation Rates and Times to Fail Following Proof Stress in Bulk Glass"; Paper 42 in Ref. 15.

[17] R. J. Charles and W. B. Hillig; pp. 511–27 in Symposium on Mechanical Strength of Glass and Ways of Improving It. Florence, Italy, September 25–29, 1961. Union Scientifique Continentale du Verre, Charleroi, Belgium, 1962.

[18] W. B. Hillig and R. J. Charles; pp. 682–705 in High-Strength Materials. Edited by V. F. Zackey. John Wiley & Sons, Inc., New York, 1965.

[19] R. E. Mould and R. D. Southwick, "Strength and Static Fatigue of Abraded Glass Under Controlled Ambient Conditions: II," *J. Amer. Ceram. Soc.*, **42** [12] 582–92 (1959).

[20] K. R. Linger and D. G. Holloway, "Fracture Energy of Glass," *Phil. Mag.*, **18** [156] 1269–80 (1968).

[21] J. E. Srawley and Bernard Gross, "Stress Intensity Factors for Crackline-Loaded Edge-Crack Specimens," *Mater. Res. Stand.*, **7** [4] 155–62 (1967).

[22] S. M. Wiederhorn, A. M. Shorb, and R. L. Moses, "Critical Analysis of the Theory of the Double Cantilever Method of Measuring Fracture-Surface Energies," *J. Appl. Phys.*, **39** [3] 1569–72 (1968).

[23] P. C. Paris and G. C. Sih, "Stress Analysis of Cracks"; pp. 30–81 in Fracture Toughness Testing and Its Applications, ASTM Special Technical Publication No. 381. American Society for Testing and Materials, Philadelphia, Pa., 1965.

[24] A. S. Tetelman and A. J. McEvily, Jr., Fracture of Structural Materials. John Wiley & Sons, Inc., New York, 1967.

[25] S. M. Wiederhorn; pp. 217–41 in Mechanical and Thermal Properties of Ceramics. Edited by J. B. Wachtman, Jr. *Nat. Bur. Stand. (U.S.) Spec. Publ.*, **1969**, No. 303; 268 pp.

[26] A. J. Holland and W. E. S. Turner, "Effect of Sustained Loading on Breaking Strength of Sheet Glass," *J. Soc. Glass Technol.*, **24** [101] 46–57T (1940).

[27] E. B. Shand, "Experimental Study of Fracture of Glass: I," *J. Amer. Ceram. Soc.*, **37** [2] 52–60 (1954).

[28] John Mandel, Statistical Analysis of Experimental Data. Interscience Publishers, New York, 1964.

[29] B. A. Proctor, I Whitney, and J. W. Johnston, "Strength of Fused Silica," *Proc. Roy. Soc., Ser. A*, **297** [1451] 534–57 (1967).

[30] J. E. Ritter, Jr., "Fatigue Strength of Silicate Glasses," *Phys. Chem. Glasses*, **11** [1] 16–17 (1970).